

# The CYGNSS Flight Segment; A Major NASA Science Mission Enabled by Micro-Satellite Technology

Randy Rose  
Southwest Research Institute  
6220 Culebra Rd  
San Antonio, TX 78238  
303-588-2157  
rrose@swri.org

Chris Ruf  
University of Michigan  
2455 Hayward  
Ann Arbor, MI 48109  
734-764-6561  
cruf@umich.edu

Debi Rose  
Southwest Research Institute  
1050 Walnut St, Suite 300  
Boulder, CO 80301  
720-240-0157  
debi.rose@swri.org

Marissa Brummitt  
Surrey Satellite Technology  
8310 South Valley Hwy  
Englewood, CO 80112  
720-545-0865  
MBrummitt@sst-us.com

Aaron Ridley  
University of Michigan  
2455 Hayward  
Ann Arbor, MI 48109  
734-764-5727  
ridley@umich.edu

**Abstract**—While hurricane track forecasts have improved in accuracy by ~50% since 1990, there has been essentially no improvement in the accuracy of intensity prediction. This lack of progress is thought to be caused by inadequate observations and modeling of the inner core due to two causes: 1) much of the inner core ocean surface is obscured from conventional remote sensing instruments by intense precipitation in the inner rain bands and 2) the rapidly evolving stages of the tropical cyclone (TC) life cycle are poorly sampled in time by conventional polar-orbiting, wide-swath surface wind imagers. NASA’s most recently awarded Earth science mission, the NASA EV-2 Cyclone Global Navigation Satellite System (CYGNSS) has been designed to address these deficiencies by combining the all-weather performance of GNSS bistatic ocean surface scatterometry with the sampling properties of a satellite constellation.

This paper provides an overview of the CYGNSS flight segment requirements, implementation, and concept of operations for the CYGNSS constellation; consisting of 8 microsatellite-class spacecraft (<100kg) each hosting a GNSS receiver, operating in a 500 km orbit, inclined at 35° to provide 70% coverage of the historical TC track. The CYGNSS mission is enabled by modern electronic technology; it is an example of how nanosatellite technology can be applied to replace traditional “old school” solutions at significantly reduced cost while providing an increase in performance. This paper provides an overview of how we combined a reliable space-flight proven avionics design with selected microsatellite components to create an innovative, low-cost solution for a mainstream science investigation.

## TABLE OF CONTENTS

1.	INTRODUCTION.....	1
2.	CYGNSS MISSION DESIGN .....	2
3.	MISSION IMPLEMENTATION.....	3
4.	DELAY DOPPLER MAPPING INSTRUMENT .	4
5.	MICROSATELLITE.....	6
6.	DEPLOYMENT MODULE .....	11
7.	CONCLUSION .....	12
	REFERENCE .....	12
	BIOGRAPHIES.....	13

## 1. INTRODUCTION

Tropical Cyclone (TC) track forecasts have improved in accuracy by ~50% since 1990, largely as a result of improved mesoscale and synoptic modeling and data assimilation. In that same period, there has been essentially no improvement in the accuracy of intensity forecasts. This fact is widely recognized not only by national research institutions [1] [2] but by the popular press as well [3].

The fact that forecast improvements in TC intensity have lagged so far behind those of TC track suggests that the deficiency lies somewhere other than proper observations and modeling of the mesoscale and synoptic environment. The Cyclone Global Navigation Satellite System (CYGNSS) will resolve the principle deficiency with current TC intensity forecasts, which lies in inadequate observations and modeling of the storm’s inner core. The inadequacy in observations results from two causes: 1) much of the inner core ocean surface is obscured from conventional remote sensing instruments by intense precipitation in the eye wall and inner rain bands and 2) the rapidly evolving (genesis and intensification) stages of the TC life cycle are poorly sampled in time by conventional polar orbiting, wide-swath imagers. CYGNSS is specifically designed to address these two limitations.

This paper is part of a coordinated series of papers being presented at the 2013 IEEE Aerospace Conference in Big Sky, MT. The full series includes:

- CYGNSS Mission overview, science objectives, and requirement allocation [Session 2.05-2532; Dr. Chris Ruf]
- CYGNSS Mission implementation with specific emphasis on the microsat [This paper, Session: 2.05]
- CYGNSS Science instrument [Session: 6.02-2410; Marissa Brummitt]
- CYGNSS Mission operations [Session: 12.02-2559; Debi Rose]

- CYGNSS Avionics implementation [Session: 7.07-2602, John Dickinson]

## 2. CYGNSS MISSION DESIGN

CYGNSS measures the ocean surface wind field with unprecedented temporal resolution and spatial coverage, under all precipitating conditions, and over the full dynamic range of wind speeds experienced in a TC. It does so by combining the all-weather performance of GPS-based bistatic scatterometry with the sampling properties of a dense microsatellite constellation. Near-surface winds over the ocean are major contributors to and indicators of momentum and energy fluxes at the air/sea interface. Our goal, to understand the coupling between the surface winds and the moist atmosphere within a TC, is key to properly modeling and forecasting its genesis and intensification.

Surface wind fields of the TC inner core, including regions beneath the intense eye wall and rain bands that could not previously be measured from space will be provided by CYGNSS. Mission simulation studies predict a mean revisit time of 4.0 hrs. The CYGNSS wind fields, when combined with as-frequent precipitation fields (e.g. produced by the upcoming Global Precipitation Measurement (GPM) core satellite and the current constellation of precipitation imagers), image the evolution of both the precipitation and underlying wind fields throughout the complete TC life cycle. They provide coupled observations of moist atmospheric thermodynamics and ocean surface response, and enable new insights into TC inner core dynamics and energetics.

The use of a dense constellation of microsatellites results in spatial and temporal sampling properties that are markedly improved from conventional wide swath polar imagers. All previous spaceborne measurements of ocean surface vector winds have suffered from degradation in highly precipitating regimes. As a result, in the absence of reconnaissance aircraft, the accuracy of wind speed estimates in the inner core of the hurricane is often highly compromised. The added quality and quantity of surface wind data provided by CYGNSS in precipitating conditions significantly improves estimates of intensity. Most current spaceborne active and passive microwave instruments are in polar low earth orbits (LEOs). The orbits maximize global coverage but can result in large gaps in the tropics [4]. The irregular and infrequent revisit times (ca. 11-35 hrs) are likewise not sufficient to resolve synoptic scale temporal variability. Missed core imaging events can occur when an organized system passes through an imager's coverage gap

or when its motion is appropriately offset from the motion of the imager's swath. One particularly egregious case is Hurricane Dean, which was sampled less than 5% of the time.

Each CYGNSS Observatory consists of a microsatellite (commonly referred to as a "microsat") platform hosting a GPS receiver modified to measure surface reflected signals. Similar GPS-based instruments have been demonstrated on both airborne and spaceborne platforms to retrieve wind speeds as high as 60 m/s (a Category 4 hurricane) through all levels of precipitation, including the intense levels experienced in a TC eyewall [5]. Each Observatory simultaneously tracks scattered signals from up to four independent transmitters in the operational GPS network. The number of Observatories and orbit inclination are chosen to optimize the TC sampling properties. The result is a dense cross-hatch of sample points on the ground that cover the critical latitude band between  $\pm 35^\circ$  with an average revisit time of 4.0 hrs.

### *Baseline Design Performance*

The performance of the baseline mission design was developed using a time-dependent overlay of the simulated CYGNSS sampling characteristics onto a database of storm tracks for every TC that occurred during the 2003-2007 Atlantic hurricane seasons. A total of 84 TCs were recorded during this period, making it an excellent population with which to determine the statistical properties of our performance. The time-dependent version of the overlay accounts for the relative orbital motion of each CYGNSS microsat and GPS spacecraft as well as the trajectory of every TC. It predicts where and when every sample of every TC would have occurred if CYGNSS had been in orbit during 2003-2007. From this data, detailed coverage statistics are derived. Parametric sensitivity analysis of the dependence of CYGNSS performance on various mission design variables was conducted using a time-independent overlay. In this case, all CYGNSS spatial samples made in a 24 hr period were overlaid onto a compiled record of all named storm tracks (with wind speeds >30 kts) from 2000-2009.

*Number of Observatories*—The 24 hr storm coverage statistic is shown in Figure 1 as a function of the number of Observatories lost from the initial constellation. The result from the time-dependent analysis – that 7 are sufficient but 6 are not – is consistent with a time-independent requirement of 70% or more 24 hr storm coverage. For this reason, the value of 70% is used as a time-independent proxy for the time-dependent requirement.

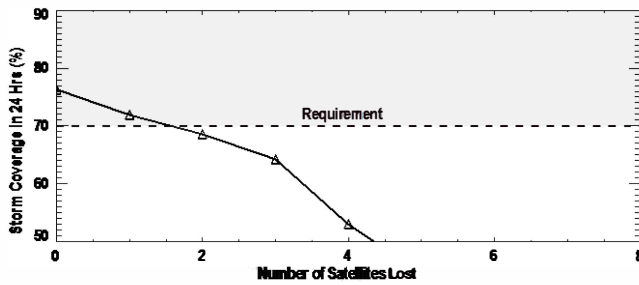


**Figure 1- Dependence of 24 hr coverage on number of Observatories lost. The 70% storm coverage requirement is met by 7 or more Observatories.**

*Orbit Altitude*—Altitude can affect coverage in competing ways. As altitude increases, the projected antenna footprint on the ground grows, increasing the potential number of observable GPS reflections. Increasing altitude also lengthens the propagation path and lowers received signal strength, thus narrowing the usable solid angle of the antenna pattern. The increase in footprint size would dominate if the number of observable reflections was allowed to grow. However, because the Delay Doppler Mapping Instrument (DDMI) can simultaneously observe a maximum of only 4 reflections, coverage does not improve much above an altitude of ~350 km. Coverage begins to decrease due to the longer propagation path above ~550 km. The baseline altitude of 500 km satisfies the mission lifetime requirement while staying within the broad range indicated by this coverage analysis.

*Orbit inclination*—Inclination affects storm coverage in two ways. Very low inclination angles reduce coverage because the prevailing latitudinal “corridors” favored by tropical storms become under-sampled or missed altogether. Inclination angles too far above these preferred latitudes also tend to decrease coverage because more time is spent over mid-latitude regions with a low probability of TC occurrence. These competing dependencies are shown in Figure 2. The baseline mission design of 35° is located at the center of a broad maximum in coverage.

### 3. MISSION IMPLEMENTATION

CYGNSS uses an innovative constellation of microsats to provide wind speed data to NASA and the Earth science community in a low-risk, cost effective manner. Dr. Chris Ruf (University of Michigan) leads the CYGNSS team as an experienced Principal Investigator with extensive science, algorithm and sensor experience. SwRI is responsible for system engineering, microsat development, system AI&T, and mission operations. Surrey is responsible for the Delay Doppler Mapping Instrument (DDMI), while Ames provides the constellation Deployment Module (DM).

The CYGNSS Mission Operation Center (MOC), managed by SwRI, the Science Operations Center/Data Archive Center (SOC/SDC), managed by UM, and Universal Space

Network (USN) ground stations form the CYGNSS ground segment (GS).

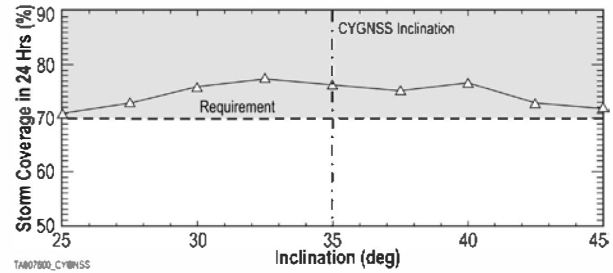


**Figure 2 - Figure E.1-3 Dependence of 24 hr coverage on orbit inclination angle. 35° baseline inclination is centered in a broad maximum of storm coverage dependence, leaving a wide margin for inclination angle variations, if needed**

CYGNSS is enabled by technology with nanosat heritage and serves as a prime example of applying a low-cost constellation to fill a gap data provided by existing monolithic observatories [6]. Mission implementation involves a simple nadir-pointed Observatory hosting an instrument technically proven on orbit. Required global coverage is provided by 8 Observatories loosely dispersed about a 500 km, 35° circular orbit. The mission profile does not require any orbit maintenance as orbit analyses indicate that spacing of the Observatory created by specific initial orbital deployment is sufficient to meet science requirements and that “clumping” of the Observatories does not occur. No attitude maneuvers are required other than recovery of initial pointing errors resulting from deployment from the launch vehicle. After commissioning and engineering operations are completed, the Observatories are placed into nominal Science mode, where they operate continuously with no instrument commanding required except for bi-annual engineering calibration operations. The simple mode flow is illustrated in Figure 3.

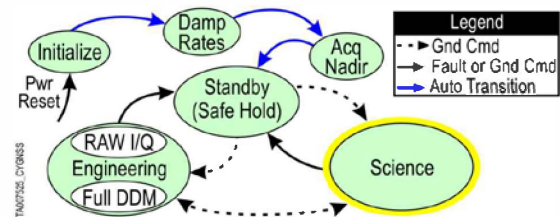


**Figure 3 - Observatory mode flow**

While the constellation is central to meeting science requirements, the individual Observatories act independent of one another, with no need to synchronize with the other Observatories. They are identical in design but provide their own individual contribution to the CYGNSS science data set. The Observatory consists of the DDMI integrated with the microsat. The Deployment Module, using coordination signals from the LV, deploys the Observatories into their

proper initial orbit configuration. The CYGNSS system is designed to reduce operational overhead of the CYGNSS Observatories during normal science operations to alleviate configuration control issues associated with standard spacecraft and provide a more efficient operational scenario for the constellation.

*Operational Concept*

*Launch and Early Operations*—The launch configuration is comprised of the 8 Observatories mounted on a DM in 2 tiers of 4 Observatories (Figure 4). The LV places the integrated constellation and DM into an orbit of 500 km circular, 35° inclination where the DM deploys the Observatories in opposite pairs to balance forces imparted on the LV control system. Separation events are spaced roughly 60 s apart to prevent local collisions. The LV orients the integrated DM-Observatory stack such that the first Observatory pair is deployed 10° cross-track. No additional LV maneuvering is required. This LV orientation, combined with the DM’s physical clocking and different separation spring forces, creates proper orbital dispersion.

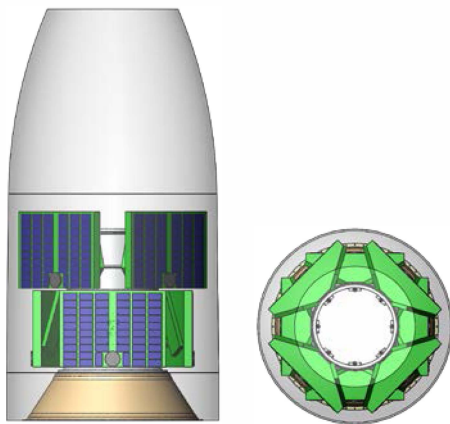


**Figure 4 - Launch configuration of the CYGNSS constellation**

The Observatories autonomously recover from any deployment tipoff rates and orient themselves into a nadir configuration within 3 orbits. They then transition into Standby mode where power margins allow the Observatory to remain indefinitely with their S/A stowed. S/A deployment is initiated via ground command during communication passes nominally within the first 14 orbits after deployment. The Observatories then enter the commissioning phase of operations where they are tested in an interleaved fashion so the constellation is ready to transition to Science operations after L+8 wks.

*Science Operations*—Following commissioning, the DDMI is set to Science mode for the duration of the mission, except for brief returns to engineering verification performed bi-annually. In Science mode, sub-sampled

DDMs are generated on-board and downlinked with 100% duty cycle. The Observatories are designed to implement nominal Observatory operations and science data collection without on-board schedule command sequences.

**4. DELAY DOPPLER MAPPING INSTRUMENT**

CYGNSS accomplishes its science goal using a Delay Doppler Mapping Instrument (DDMI) on each Observatory. The CYGNSS DDMI uses Surrey’s off-the-shelf GNSS Receiver-Remote Sensing Instrument (SGR-ReSI), an upgraded version of the UK-DMC-1 instrument that flew in 2003. The upgrades include a new GPS front end MMIC receiver and the addition of a digital signal processing back end. The new front end improves noise performance, adds internal calibration, and raises the digital sample rate. The new back end adds more on-board processing capacity in order to raise the duty cycle of science operations.

In total, the DDMI consists of the Delay Mapping Receiver (DMR) electronics unit, two nadir-pointing antennas for collecting reflected GNSS signals, and a zenith-facing antenna providing space-geolocation capability.

DDMI onboard processing generates maps of GPS signals scattered from the ocean surface. These are referred to as Delay Doppler Maps (DDMs). The coordinates of a DDM are Doppler shift and time delay offset relative to the specular reflection point of the GPS signal. Each pixel of the DDM is obtained by cross-correlation of the received signal with a locally generated replica time delay and Doppler shift. An open-loop tracking algorithm allows each DDM to be processed by predicting the position of the specular reflection point from the known positions of the receiver and GPS transmitter. The entire data flow is shown in Figure 5. Each DDM has 128 delay pixels with resolution of 61 ns. The Doppler resolution is 250 Hz over a ±6.5 kHz range, resulting in 52 Doppler pixels.

Available hardware resources allow generation of four simultaneous DDMs. The output data rate is determined by onboard coherent and incoherent integration. The coherent (complex signal) integration time is limited to 1 ms by the rate of change of the propagation geometry due to receiver motion. Individual complex DDMs are then incoherently integrated (magnitude only) for 1 s to form the final DDM. Incoherent integration reduces noise due to speckle and improves the signal-to-noise ratio (SNR). The incoherent integration time is limited to 1 s due to the degradation in spatial resolution caused by along-track smearing.

*Instrument Accommodation*

While not challenging, instrument accommodation and LV compatibility requirements are used to drive the microsat element requirements, resulting in an integrated microsat-DDMI solution that meets all science requirements and allows use of the available NASA NLS-II launch services.

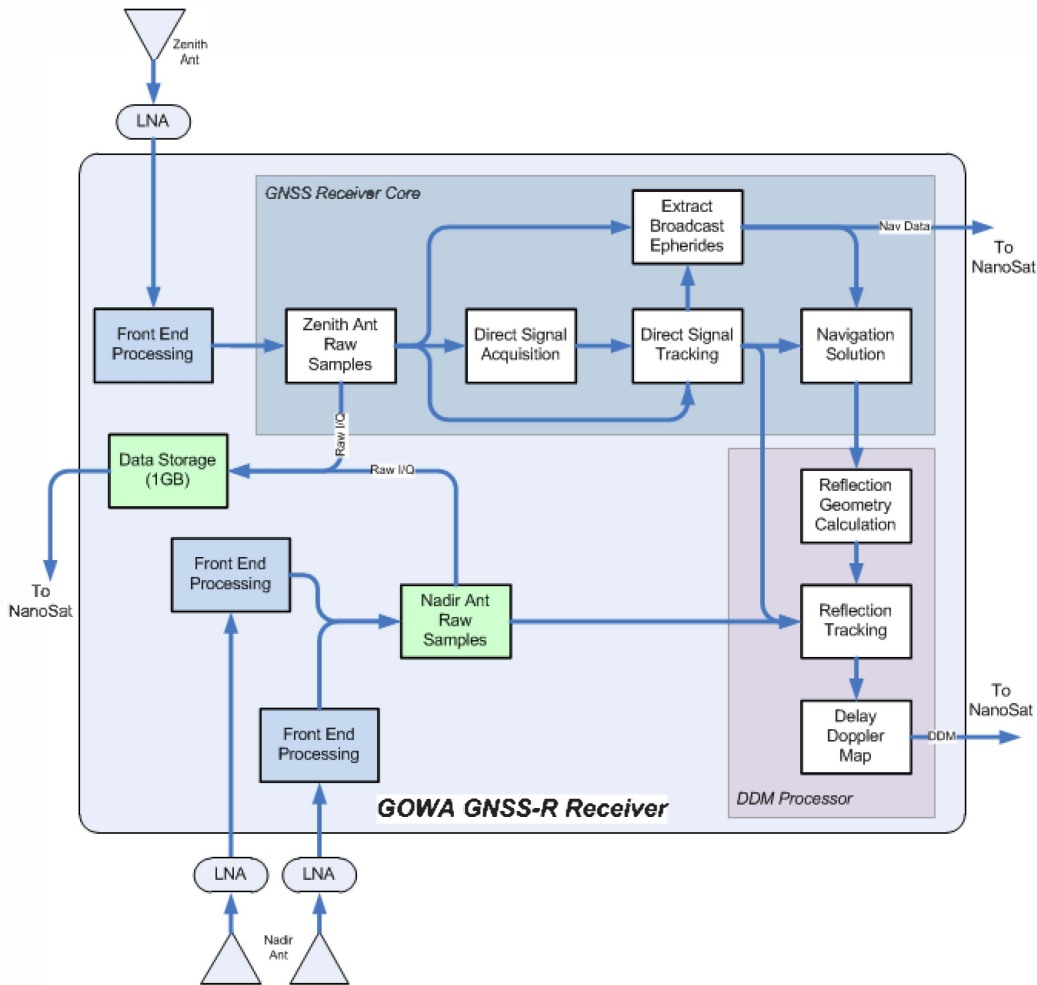


**Figure 5 - DDMI data flow diagram**

*Configuration*—DDMI antenna pointing constraints drive the overall Observatory physical configuration. The dependence of science coverage requirements on the tilt and rotation pointing angles of the antenna boresight was determined using the CYGNSS mission simulator. Figure 6 illustrates that the dependence of storm coverage on antenna tilt, or roll about the x-axis, is minimal. Figure 7 shows that the coverage dependence on antenna rotation, or yaw about the z-axis, is also minimal. A wide range of antenna configurations were analyzed to meet the science requirements for 70% 24 hr storm coverage with a <12 hr mean revisit tempo. A tilt angle of 28° and rotation angle of 60° were chosen to optimize Observatory close packing and accommodation on the Deployment Module (DM) during launch. The relative insensitivity of spatial coverage to antenna pointing relaxes several other requirements. Mechanical tolerances on the alignment between the electrical boresight of the antenna and the optical boresight of the attitude determination sensor can be relaxed, as can the control of the microsat attitude itself while on orbit.

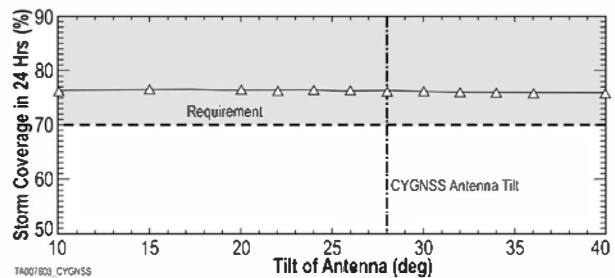


**Figure 6 - Antenna tilt analysis demonstrates design trade space to accommodate manufacturing tolerances and performance improvements if necessary**

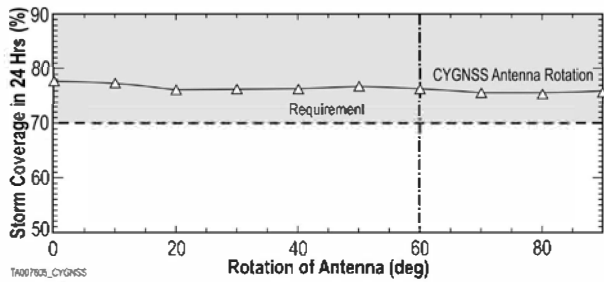


**Figure 7 - Antenna rotation analysis results illustrate key configuration decision effects on science performance**

*Pointing*—Pointing knowledge uncertainty directly translates into an uncertainty in the antenna pattern gain in the direction of the specular reflection point producing an uncertainty in calibration of the scattering cross-section needed to estimate wind speed. Given the science requirement for wind speed error of  $<2$  m/s or 10% of the wind speed (whichever is greater), we have allocated 65% of the error budget as the pointing knowledge requirement to accommodate other physical error sources. A pointing knowledge uncertainty requirement of  $2.7^\circ$  ( $3\sigma$ ) translates into a max absolute error of 0.8 m/s for wind speeds below 20 m/s and a 6.2% max relative error for wind speeds between 20 and 60 m/s (Figure 8).

Pointing control is not critical with primary considerations derived from providing a nadir reference and minimizing signal path loss due to cosine losses. We conservatively require  $5^\circ$  ( $1\text{-}\sigma$ ) control of antenna pointing relative to microsat nadir.

Pointing stability and jitter requirements are derived from the DDM processing requirement. The DDM is formed by coherent integration over 1 ms, followed by incoherent averaging of 1000 DDMs to improve SNR. The coherent integration requires that the image be stable to 1/10 the order of the DDM resolution, whereas the incoherent integration requires pointing stability on the order of the resolution. The spatial extent of the DDM covers  $\sim 100 \times 100$  km and is sampled every 1 km. The nominal range of  $\sim 1000$  km from the Observatory to the specular reflection point corresponds to a subtended angle of 0.001 radian/pixel. The pointing jitter is required over a coherent integration time (1 ms) to be no more than 1/10 of the pixel size ( $20''/\text{ms}$ ), and the stability over the incoherent integration time (1 s) is required to be no more than one half the pixel size ( $100''/\text{s}$ ). As a result, the short term pointing jitter has a negligible effect on the science data processing.

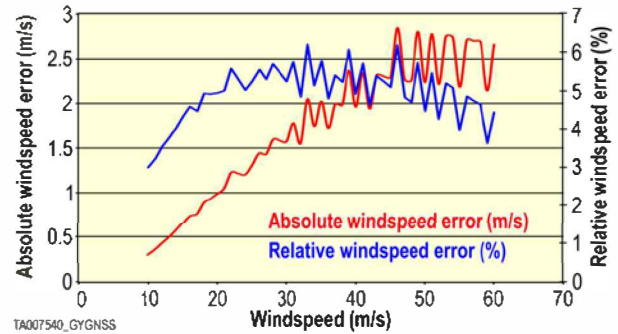


**Figure 8 - Wind speed error due to  $2.7^\circ$  ( $3\sigma$ ) pointing knowledge uncertainty**

*On-board Data Handling*—The CYGNSS mission is enabled by the DDMI capability to convert raw I/Q data to Delay Doppler Maps (DDM), but even the heritage DDM processing requires further on-board data volume reduction to meet downlink limitations of the microsatellite. The fully resolved DDM from the DDMI contains many highly correlated image pixels, as well as many pixels that do not contain information about the local wind field in the scattering region. In order to reduce the downlink data rate, an onboard image sub-sampling algorithm is used prior to data downlinking providing a 80:1 reduction in the DDM data size, resulting in a total data downlink volume of 56.2 MB/1.5 days. The DDMI also outputs CYGNSS Observatory ephemerides for microsat position knowledge and GNSS ephemerides for DDM geo-referencing.

*Power*—The DDMI requires 10 W at 28 V for science data collection. Stand-by mode is not necessary as the unit can be turned off while not in use and requires minimal warm-up time when powered ON. Data collection starts after  $\sim 5$  min, when the unit has acquired the necessary GPS satellites.

## 5. MICROSATELLITE

The CYGNSS Observatory is based on a single-string hardware architecture (Figure 9) with functional and selective redundancy included for critical areas. The microsat has been designed from the beginning for ease of manufacture, integration, and test to provide a low-risk, cost-effective solution across the constellation. Margins and additional characteristics are provided in Table 1 and Table 2.

### *Structure, Mechanisms, and Thermal (SMT)*

SMT subsystem design leverages SwRI's instrument and avionics SMT heritage and capabilities to meet SMT requirements.

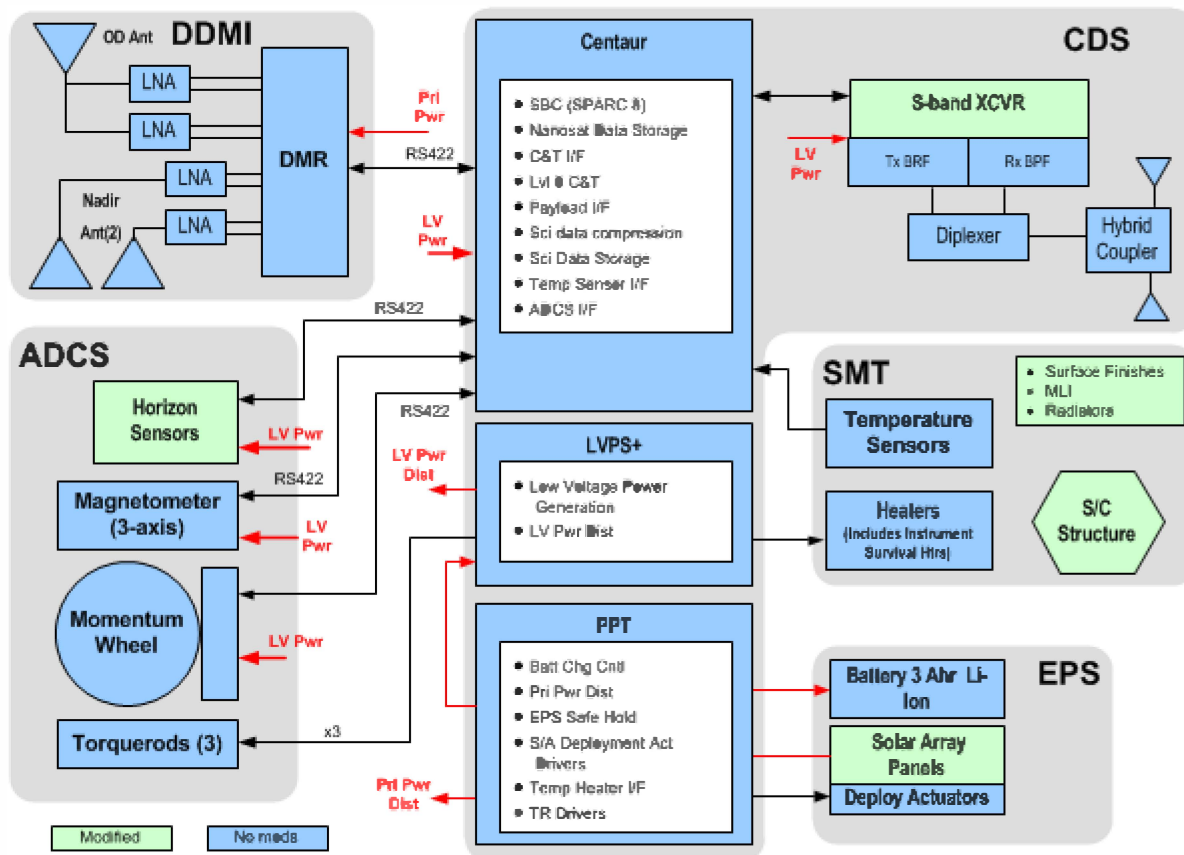


Figure 9 – CYGNSS single-string architecture

*Structure*—The microsat structure requirements are driven by physical accommodation of the DDMI antennas, the S/As, and launch configuration constraints. Our design uses the same principles as our heritage avionics chassis, using milled Al piece parts bolted together to provide an integrated, mass efficient solution for CYGNSS. Close tolerance pins/holes ensure repeatability of structural alignment. The microsat’s shape is specifically configured to allow clear nadir and zenith FOV for the DDMI antennas, while its structure integrates the microsat and instrument electronic boards directly by creating avionics and Delay Mapping Receiver (DMR) “bays” (Figure 10). The design has been coordinated with our avionics teams to ensure structural, thermal, EMI/EMC, and radiation requirements are met. The avionics and DMR bays form the core of the microsat; all other components are mounted to this backbone with structural extensions included to accommodate the Al honeycomb-based S/As and DDMI nadir antenna assemblies. The structural configuration allows easy access to all Observatory components when the nadir DDMI antenna panel assemblies and microsat endplates are removed for Observatory AI&T.

The microsat primary structure’s nadir baseplate is the DM mechanical interface for launch. Primary shear and axial loads are carried by the microsat primary structure, providing full compliance with the dynamic launch vehicle envelope. Preliminary FEA of the Observatory (Figure 11)

Table 1 - CYGNSS flight segment resource margins

Resource	Requirement	Performance (MEV)	Margin
Observatory Mass	≤28kg	≤17.6kg	59%
Spacecraft Mass	≤25kg	≤15.5kg	61%
Instrument Mass	≤3kg	≤2.1kg	43%
Deployment Module Mass	≤75kg	≤33.5kg	124%
Flight Segment Launch Mass	≤360kg	≤174.6kg	106%
Total Orbital Power (avg EOL)	≥48.8W	≥70.1W	30%
RF Downlink	≥3dB	≥6.7dB	
Science Data Downlink (avg/pass)	≥56.2MB	≥78.1MB	28%
Science Data Storage (10 days)†	≥370MB	≥4000MB	91%
Pointing Knowledge (3σ)	2.7deg	2.1deg	29%
Pointing Control (3σ)	5deg	2.8deg	79%
S/C Attitude Stability	100°/sec	26°/sec	285%
S/C Attitude Jitter	20°/1msec	1°/1msec	1900%
Agility - 5deg/sec (tipoff)	3 orbits	1.5 orbits	100%

**Table 2 - CYGNSS microsat characteristics**

Parameter/Item		Value
Radiation Total Dose		>5 krad (RDM: 2)
Design Life		2 yrs
Attitude Determination		Earth horizon and mag field reference
	Horizon Sensor	0.5 deg accuracy, ±5 deg range
	Magnetometer	10 nT sensitivity, +/- 50,000 nT range
Attitude Control		3-axis stabilized, momentum biased
	Mom Wheel	30 mNms @ 5600 rpm, 2mNm torque
	Torque Rods	1 Am <sup>2</sup> , residual moment < 0.1 Am <sup>2</sup>
Solar Array	Type and size	Fixed, 6 rigid panels, 0.22 m <sup>2</sup>
	Deployment	One-time locking release
	Cell Type	Triple junction (InGaP/InGaAs/Ge)
	Cell Eff (EOL)	28.50%
Battery	Type & capacity	Li-ion, 3.0 Ahr total (2 @ 1.5Ahr)
	DOD-EOL, worst-case	19.30%
Thermal control		Heaters, MLI, surface finishes
Comm	Uplink	S-band 125-2kbps
	Downlink H/K	S-band 1kbps-64kbps
	Downlink Sci	S-band 1.25Mbps

results predict launch loads are well within allowable material stress levels with a first mode natural frequency of 211 Hz in the launch configuration, avoiding harmonic coupling with the LV natural frequency of 75 Hz during launch. The FEA stress plot in Figure 11 assumes launch conditions using the worst combined levels from Pegasus.

*Mechanisms*—Observatory mechanisms are limited to heritage S/A deployment devices. The four “z-fold” S/A panels perform a one-time deployment as depicted in Figure 12 into a permanently locked position planar with the fixed center panels. The S/As are held in place for launch using a cup/cone interface and deployed by a combination of flight-proven TiNi Aerospace Frangibolt actuators and Sierra Nevada Corp. S/A single-axis, locking, spring-loaded hinges.

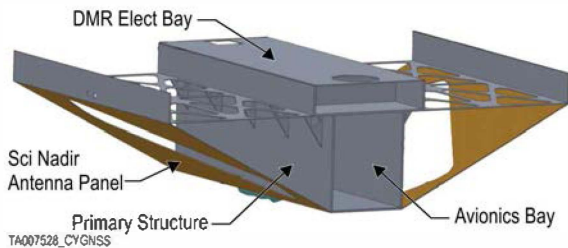


**Figure 10 - Structural element detail**

*Thermal*—The CYGNSS Observatory thermal design meets requirements to maintain all components within their temperature limits during all operational modes by using SwRI’s flight-proven, well-characterized, thermal design

techniques. The thermal control design provides thermal stability and minimizes thermal gradients through an integrated design of multilayer insulation blankets (MLI), surface treatments, and localized radiators. The arrangement of internal equipment is used to aid thermal control and eliminate the need for supplemental heaters except for Standby/Safe Hold operations.

Results from our thermal analysis were used to size the thermal radiators (EOL). The primary radiator is located on zenith surface in the S/A gap along the Observatory centerline, with a second radiator on the nadir baseplate. These locations are chosen to provide a direct, cohesive thermal conductive path to the primary observatory dissipative loads. The radiators are coated with 5 mil ITO/Tef/Ag, while MLI is used on non-radiating external surfaces. All materials used in the thermal design are flight qualified and compatible with the minimal CYGNSS contamination control requirements. Thermal radiation properties and associated degradation

factors due to the space environment are well known and included in our thermal model.

*Electrical Power Subsystem (EPS)*

The EPS is designed to perform battery charging without interrupting science data acquisition. It is based on a 28±4 Vdc primary power bus with electrical power generated by a 8-panel rigid S/A (Figure 12). The 0.71m<sup>2</sup> total area S/A provides a 30.3% margin during max eclipse periods (35.8 min). Full mission duration simulations were performed to analyze worse case solar Beta cases (±58°). The design provides 43.4% margin during these periods. When stowed, the z-fold design of the S/A allows the solar cells to face outward, combining with the two supplemental ram/wake S/As to power the microsat indefinitely in Standby mode before S/A deployment (22% margin).

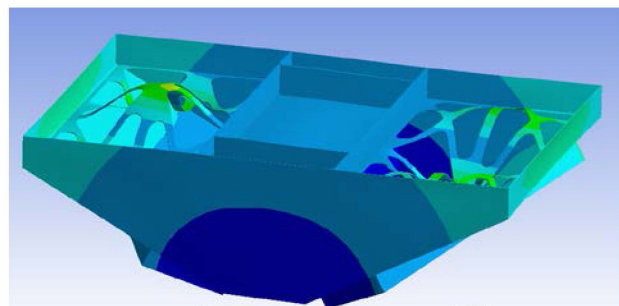


**Figure 11 – FEM/FEA results identify CYGNSS microsat 1<sup>st</sup> Freq of 211Hz**

Electrical power storage for eclipse operations is provided by 2 ABSL 1.5 A-hr Li-ion 8s1p batteries connected directly to the primary power bus. The batteries are “build-to-print” and configured for 3 A-hr (EOL) at 28.8 V nominal. Temperature sensors, and bypass diodes (to withstand a failed cell) are included in the battery assembly. ABSL battery performance models were used to analyze the CYGNSS mission with predicted EOL nominal battery state-of-charge being 87.6%.

Battery charging uses a constant current, voltage-temperature limited charge scheme based on four stored profiles matched to the CYGNSS battery. These profiles are determined during Phase B as part of the battery procurement tasks. Charging is also Coulomb limited to 120% of discharge level. The primary power bus voltage is modulated to maintain charge current and termination voltage. The Coulombic charge limit is tracked with an A-min integrator and when the level exceeds  $1.2 \times I_{dis} \times T_{eclipse} (A \cdot min)$ , battery charging levels are reduced to C/100.

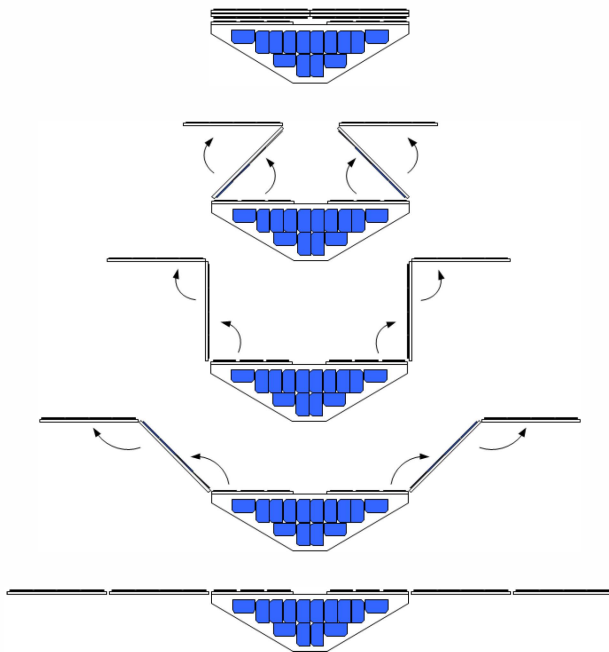


**Figure 12 – CYGNSS “z-fold” solar array provides exposed array while stowed and a balanced deployment to full power**

Battery charge regulation for the CYGNSS EPS is a peak power tracking (PPT) type regulator. The PPT board, developed using SwRI internal funds, matches S/A conductance to the Observatory load through pulse-width modulation (PWM) using an optimization control circuit that integrates S/A W-sec over a preset period of time. The PPT (located in the avionics bay) includes a GSE interface that serves as the connection point for ground power and battery maintenance, conditioning, and pre-launch trickle charging.

The EPS battery charging and power distribution hardware operates independent of flight software (FSW) except for configuration commanding and status reporting. Over-current protected switched power services are provided for the DDMI and initial microsat power application.

#### *Communications and Data Subsystem (CDS)*

The CDS meets the requirements of the CYGNSS Observatory on-board data handling and command and telemetry (C&T) communication link. Most hardware to implement the CDS resides within the CYGNSS avionics bay, with the exceptions of the S-band antennas, diplexer, and hybrid. All on-board microsat processing is performed on SwRI’s Centaur board. The Centaur consists of our space-qualified heritage Atmel SPARC8 processor with heritage CCSDS compliant C&T interface, instrument data interface, and ADCS interface designs. The board architecture is based on the Juno JADE IPB (launched Aug 2011) and extensively reuses the C&T circuitry from Deep Impact, Orbital Express, Kepler, and WISE.

The simple operational nature of the DDMI and science profile allows the CDS to be designed for autonomous control during all normal science and communication operation using only on-board Level 0 command capabilities of the Centaur, stored command sequences, and CCSDS File Delivery Protocol (CFDP) processes. Engineering operations require standard command services provided by our hardware-based heritage designs located on the Centaur. Command services include COP-0 uplink command processing with BCH error detect and correction. The Centaur also provides FSW-independent execution of a Level-0 command set used for ground-based fault management. All other commands are passed to the FSW Command Manager for execution or to the Stored Command Sequence Manager as onboard Absolute and Relative Time Sequences.

The FSW Telemetry Manager provides collection and high-level formatting of housekeeping data. These data are either downlinked in real-time or passed to the FSW Storage Manager to be stored for later downlink. Table 3 defines daily on-board data quantities and margins. The Storage Manager software controls data acquisition, recording, and playback of housekeeping and science data using the 4 GB on-board memory for data storage. The heritage 4 GB Flash memory data store allows for >10 days of continuous science operations without downlink, providing significant margin for contingency operations. A heritage hardware formatter from Orbital Express and WISE forms CCSDS source packets into transfer frames and supports four separate Virtual Channel (VC) buffers to enable optimized data routing and processing within the CYGNSS Ground Data System.

**Table 3 - CYGNSS datalink definition**

Item	Qty	Comments
Raw DMR DDM size	0.053	Mbits, DDM is 128x52 8bit
Compression	80	80:1
Stored DDM (CBE)	0.0007	Mbits
#DDM/sec	4	
DMR-S/C transfer data rate	213	kbps
Daily DDM storage (with 30% contingency)	28.8	MBytes
Allocated Daily Hskg data storage (includes 30% contingency)	8.2	MBytes, includes Sci meta data
Allocated Daily data storage total	37.0	MBytes
CCSDS overhead (14%)	5.2	MBytes
Total daily data downlink	42.1	MBytes
Downlink cadence	32.0	Hours between pass
Total data downlink/pass	56.2	Mbytes
Average downlink duration	470	sec
Required data downlink rate	0.90	Mbps
Actual data downlink rate	1.25	Mbps
Max data downlink	73.4	MBytes'@ 1.25Mbps
Downlink margin	31%	

S-band communication links are provided to uplink command sets and downlink science and housekeeping data. These links use two fixed omni-directional micro-strip patch antennas, one on the nadir baseplate and one on the zenith panel, to provide near  $4\pi$  sr communications without interrupting science operations. Normal communications use the nadir antenna, while the zenith antenna is provided for anomalous pointing.

The S-band transceiver is a single card communication solution developed by SwRI to provide a low-cost, radiation-tolerant, communication system. The core of the transceiver is a Software Defined Radio architecture configured to provide S-band (2 GHz) communications. The transceiver provides O-QPSK encoded transmit data at 1.25 Mbps with a FSK uplink receiver supporting data rates to 64 kbps.

*Attitude Determination and Control Subsystem (ADCS)*

The CYGNSS ADCS is based on a standard nadir-pointing, 3-axis, momentum-bias design using pitch/roll horizon sensors and a 3-axis magnetometer for attitude determination with a pitch momentum wheel and 3-axis torque rods providing attitude control (torque rods also provide momentum wheel desaturation). The only attitude “maneuver” required by CYGNSS is to recover from DM separation tipoff rates and establish a nadir-pointing configuration, allowing an extremely simple mode flow (Figure 13). Margins and additional characteristics are provided in Table 1 and Table 2.

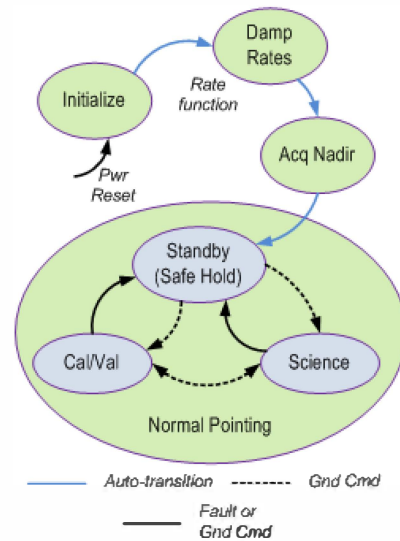


**Figure 13 – ADCS simple 3-state mode diagram aligns with the CYGNSS Observatory mode diagram**

The ADCS has three primary states of operation: rate damping, nadir acquisition, and normal pointing. The rate damping state is used initially after separation from the LV and for anomaly recovery if rates exceed normal state capabilities. Rate damping uses a “B-dot” algorithm to command magnetic dipole moments opposed to the rate of change of the magnetic vector, both measured in body coordinates. It only uses the sensed magnetic field, and does not rely on a correct orbital ephemeris or magnetic field model. Wheel speed is off for launch and initial tip-off recovery, or set to its nominal value during anomaly recovery.

After the body rates are damped, the system transitions into nadir acquisition, which monitors the pitch/roll horizon sensors to determine a rough Earth vector. The sensors are not assumed to be in their linear range; simple “on-Earth” and “off Earth” measurements are used to establish slow roll and pitch rates to bring the sensors into their linear range ( $\pm 5^\circ$ ). The momentum wheel is also maintained relatively close to its commanded nominal speed, with a desaturation gain much lower than normal.

When the ADCS brings the sensors within their linear ranges, it transitions to normal operations. The normal state uses pitch and roll measurements from the horizon sensors to calculate pitch, roll, and filtered roll rate information. It compares the measured magnetic field with a calculated model to determine yaw and filtered yaw rate information. These measurements are used to control momentum wheel torques for pitch and the electromagnets for roll and yaw angle, and pitch wheel desaturation.

Normal control is capable of degraded operation (used in Standby mode) if the ephemeris and magnetic field model are temporarily unavailable. Pitch and wheel desaturation are controlled as before, but roll and B-dot (y axis)

information are used to control roll and yaw with slightly degraded accuracy. The torque rod commanding is synchronized to permit accurate measurement of the local geomagnetic field. A Kalman filter is used to estimate body rates and improve yaw attitude estimation. Orbit position is provided via GPS determination from the DDMI.

#### *Automated Event Recognition (AER)*

On-board AER allows the CYGNSS Observatory to autonomously perform science operations while ensuring all subsystems operate within their safety limits. If subsystem data exceeds the predefined safety constraints, AER performs the designed response. The Standby mode (Figure 3) doubles as Safe Hold mode where the DDMI is powered off, providing 65% power margins to address anomalous conditions. Autonomous and on-board fault management responses are implemented using simple telemetry monitoring logic and stored command sequence capabilities. The heritage Centaur hardware design includes Watchdog provisions to monitor processor and FSW operations in addition to Level 0 command and telemetry capabilities that allow operators to monitor Observatory low level status and issue primary commands to reset the processor and shed power loads.

The Level 0 command capability is used to implement communication passes by monitoring for 30 s of ground station command carrier, which triggers an on-board stored command sequence to activate the Observatory transceiver. The ground station then implements a command procedure stored at the ground station to transfer the Observatory stored data via CFDP. The ground station then commands the Observatory transmitter off. A fault monitor automatically turns off the transmitter after 720 s.

## 6. DEPLOYMENT MODULE

The DM serves as the constellation carrier during launch and then deploys the Observatories into their proper orbital configuration once on orbit.

#### *DM Structure*

The DM consists of 2 AL cylindrical sections or tiers, each with 4 mounting/separation assemblies (Figure 14). The tier design approach simplifies Observatory-DM integration by enabling easy access of GSE while minimizing potential for damage inherent in a single core structure. The mounting/separation assemblies are positioned 90° apart to release the Observatories in pairs opposite each other, balancing deployment forces and keeping disturbance torques well within LV capabilities. Tier 2 is clocked 45° from Tier 1 to provide proper orbital dispersal vectoring.

Deployment is initiated using flight-proven, high-reliability Frangibolts. Observatory separation tip-off errors are minimized by averaging 4 push springs (Figure 14) to reduce microsat cg location criticality and minimize the effects of spring tolerances. Tip off errors are further

reduced by screening the springs during DM assembly. Each Observatory is secured to the DM by torquing the Frangibolt actuator into the microsat nadir baseplate, compressing the separation springs to achieve desired spring load for Observatory ejection. Tapered alignment pins, combined with the Frangibolt actuator, rigidly constrain each Observatory to the DM for launch. Preliminary FEM quasi-static load analysis of the fully integrated FS indicates that launch loads have a 2.17 safety factor against ultimate loads. The FEA also indicates the first natural frequency of the structure is a radial mode (Lobar) at 47.6 Hz in the launch configuration, avoiding harmonic coupling with the LV during launch.

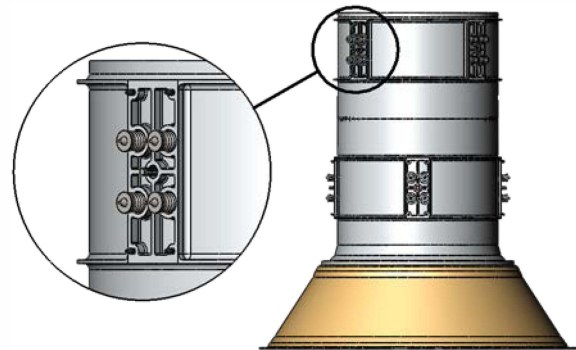


**Figure 14 – 2-tier Deployment Module provides balanced separation forces by using a matched spring deployment mechanism**

#### *DM Avionics*

The DM uses a heritage electronic sequencer to release the Observatories in a pre-determined sequence stored within the sequencer memory. The sequence is initiated via a standard LV discrete signal when the LV arrives at the required orbit. The sequencer then performs the deployment sequence by actuating the Frangibolt actuators. Sequence timing incorporates constellation separation requirements and deployment actuation tolerances. Hardware safety is ensured through the use of a 2-stage command, single-fault tolerant actuator driver design that includes a pre-flight Safe/Arm connector to fully disarm the system.

A 28 Vdc DC 140 W-hr Li-Ion battery is used to power the DM avionics and activates the deployment Frangibolt actuators. The battery is fully charged at launch with <5% of capacity required to complete the orbit insertion and deployment sequence.

In support of pre-launch operations, the DM avionics route Observatory battery trickle charge power from the GSE to the Observatory via separation connectors, with battery temperature signals acquired by the DM avionics and routed to the GSE for monitoring (Figure 15). Pre-launch Observatory command and telemetry handling is also provided by the DM avionics. The GSE command data stream is routed to each Observatory command hardline

interface with only buffering provided by the DM. Specific command targeting is a function of S/C ID; the Observatory ignores the command if the S/C ID is not applicable. The DM enables Observatory pre-launch health and status monitoring by multiplexing the Observatory hardline telemetry.

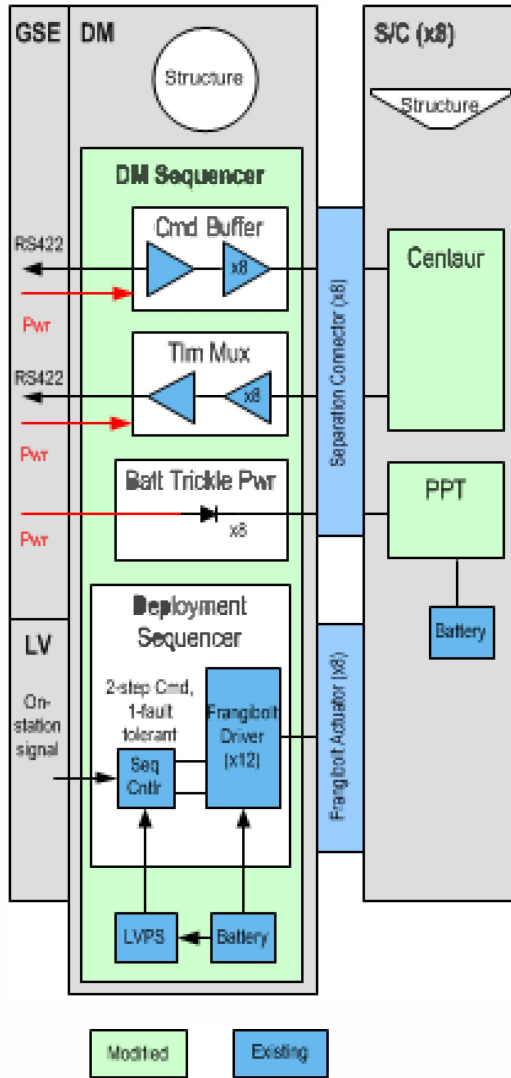


**Figure 15 – Deployment Module block diagram illustrates its Pre-Launch and Launch functionality**

## 7. CONCLUSION

The CYGNSS mission implementation provides strong resiliency to unforeseen issues: reduced NRE using many “build-to-print” components, a simple Observatory operational concept allows mission operations to focus on monitoring the constellation; and system level redundancy that provides inherent fault tolerance and graceful system degradation/fault tolerance with only 7 of 8 Observatories required for baseline science. Our design is specifically tailored for a straightforward, cost-effective AI&T campaign, while strong contingencies and margins for all

resources allow flexibility to solve issues without compromising science goals.

The CYGNSS mission introduces a new paradigm in low-cost Earth science missions that employs a constellation of science-based microsats to fill a gap in capabilities of existing large systems at a fraction of the cost. CYGNSS will provide unprecedented coverage of winds within a TC throughout its life cycle thus providing critical data necessary for advancing the forecast of TC intensification.

## REFERENCE

- [1] N. S. Foundation, "Hurricane Warning: The Critical Need for a National Hurricane Research Initiative, NSB-06-115," 2007.
- [2] National Oceanic and Atmospheric Administration, "Hurricane Forecast Improvement Project," 2008.
- [3] S. Borenstein and C. Amario, "Irene forecasts on track; not up to speed on wind," Associated Press, 2011.
- [4] M. Schlax, D. B. Chelton and M. H. Freilich, "Sampling Errors in Wind Fields Constructed from Single and Tandem Scatterometer Datasets," *Journal of Atmospheric and Oceanic Technology*, pp. 18, 1014–1036, 2001.
- [5] S. Katzberg, R. A. Walker, J. H. Roles and T. Lync, "First GPS signals reflected from the interior of a tropical storm: Preliminary results from hurricane Michael," *Geophysical Research Letters*, vol. 28, pp. 1981-1984, 2001.
- [6] R. J. Rose, J. Dickinson and A. Ridley, "CubeSats to NanoSats; Bridging the Gap between Educational Tools and Science Workhorses," in *IEEE Aerospace Conference*, Big Sky, Montana, 2012.

## BIOGRAPHIES



**Randy Rose** received a B.S. in Engineering from the South Dakota School of Mines and Technology in 1980. Mr. Rose is a staff engineer for SwRI Space Systems Division where he serves as a lead for spacecraft systems development. He has more than 30 years of experience in the spacecraft development community with experience in all aspects of spacecraft development including project management, systems engineering, computer architecture, ADCS, hardware and software design, I&T, and operations. His experience includes hands-on hardware development experience with all spacecraft subsystems. Mr. Rose is the NASA CYGNSS Project Systems Engineer responsible for the development of the overall CYGNSS system and microsat designs.



**Chris Ruf** received the B.A. degree in physics from Reed College, Portland, OR, and the Ph.D. degree in electrical and computer engineering from the University of Massachusetts, Amherst. He is currently a Professor of atmospheric, oceanic, and space sciences and Director of the Space Physics Research Laboratory at the University of Michigan, Ann Arbor. He has worked previously at Intel Corporation, Hughes Space and Communication, the NASA Jet Propulsion Laboratory, and Penn State University. In 2000, he was a Guest Professor with the Technical University of Denmark. He has published in the areas of satellite microwave radiometry and atmospheric, oceanic, land surface and cryosphere retrieval algorithms. Dr. Ruf is a member of the American Geophysical Union (AGU), the American Meteorological Society (AMS), and Commission F of the Union Radio Scientifique Internationale. He has served on the editorial boards of AGU Radio Science, the IEEE Transactions on Geoscience and Remote Sensing (TGRS), and the AMS Journal of Atmospheric and Oceanic Technology. He is currently the Editor-in-Chief of TGRS. Dr. Ruf is the Principal Investigator of the NASA CYGNSS mission.



**Debi Rose** received a B.S. in Electrical Engineering from Arizona State University, Tempe AZ in 1982 and a M.E. in Engineering Management from the University of Colorado, Boulder CO in 1995. She has been with Southwest Research Institute for 5 years. Prior to joining SwRI, she worked in various system engineering and project management roles in both the

aerospace and telecommunications industry at Motorola, Ball Aerospace, Intel, and several start-up companies. Ms Rose is the NASA CYGNSS Mission Operations Manager, responsible for the overall development and operations of the CYGNSS Ground Segment.

**Marissa Brummitt** received her B.S. and M.S. in Aerospace Engineering from California Polytechnic State University San Luis Obispo (2010). Since 2006, Ms. Brummitt has gained nanosatellite integration and test experience at Cal Poly San Luis Obispo and the Naval Postgraduate School (NPS). At Cal Poly she participated in the CubeSat program, specifically in the area of vibration testing of the Poly Picosatellite Orbital Deployer (PPOD). At NPS, within the Space Systems Academic Group, she was the lead test engineer for the Solar Cell Array Tester (NPS-SCAT) CubeSat and completed a Master's thesis based on the vibration qualification of the spacecraft and a next generation Cal Poly vibration TestPod. At Surrey Satellite Technology US LLC Ms. Brummitt is a Systems Engineer supporting system design for proposals, studies and missions. As part of the CYGNSS team she is the Delay Doppler Mapping Instrument Systems Engineer.



**Aaron Ridley** received his B.S. in Physics from Eastern Michigan University (1992) and his Ph.D. in Atmospheric, Oceanic and Space Science from the University of Michigan (1997). Dr. Ridley worked at SwRI after graduation, and returned to UM in 2000. He is primarily a computational researcher who utilizes large-scale simulations to better understand the near-Earth space environment. He is the PI of the CADRE CubeSat, which will measure the thermospheric and ionosphere density, temperature and winds. He is also the PI for a Fabry-Perot Interferometer, deployed in Michigan and the engineering portion of an autonomous flux gate magnetometer array deployed in Antarctica. Dr. Ridley is the Instrument Scientist for the NASA CYGNSS mission.